



Cite this: *Chem. Commun.*, 2023, 59, 12899

Received 18th September 2023,  
Accepted 4th October 2023

DOI: 10.1039/d3cc04583h

[rsc.li/chemcomm](http://rsc.li/chemcomm)

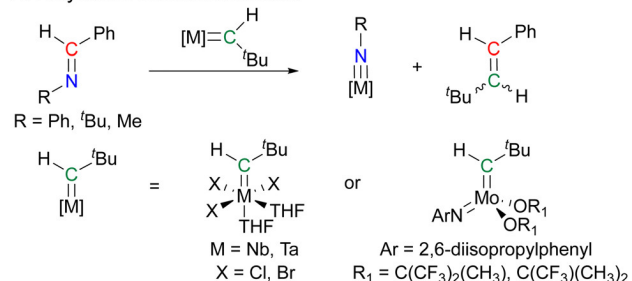
**Reactions between imines and tungsten alkylidyne complexes are studied. The trianionic pincer ligand supported alkylidyne [<sup>t</sup>BuOCO]WCC(CH<sub>3</sub>)<sub>3</sub>(THF)<sub>2</sub> (**1**) reacts with *N*-(R)-1-phenylmethanimine (PMI-R, R = Me, Ph, Bn, and TMS) yielding [<sup>t</sup>BuOC(H)O]W( $\eta^2$ -<sup>t</sup>BuC≡CPh)N(R) (**4-R**), products from metathesis reaction. In contrast, the non-pincer alkylidyne (<sup>t</sup>BuO)<sub>3</sub>W≡CC(CH<sub>3</sub>)<sub>3</sub> does not react with PMI-R imines.**

Imines participate in metathesis-like reactions. Imine-imine metathesis<sup>1–4</sup> is the exchange of NR/CHR groups between different imines and is a synthetic tool for carboamination of alkynes,<sup>5,6</sup> metal organic polyhedra,<sup>7</sup> covalent adaptable networks,<sup>8</sup> and self-healing polymers<sup>9</sup> and copolymers.<sup>10</sup> Imines slowly undergo metathesis without a catalyst but metal-imido complexes accelerate the exchange.<sup>5,11–17</sup> Access to a four-membered metallacycle intermediate,<sup>4,5,18</sup> similar to that of alkene and alkyne metathesis,<sup>19</sup> lowers the kinetic barrier.<sup>20,21</sup> Metal alkylidenes also react with imines in stoichiometric metathesis reactions.<sup>22–27</sup>

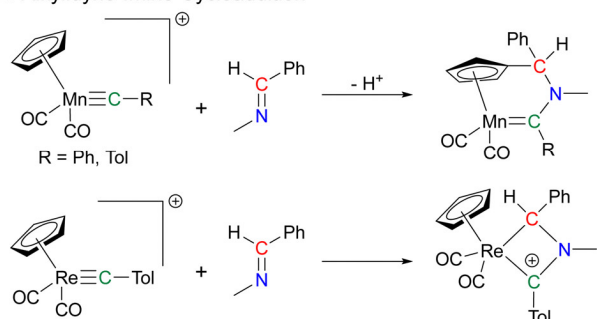
Scheme 1A depicts examples of Nb, Ta and Mo alkylidenes in irreversible metathesis with imines yielding new alkenes and metal-imido complexes.<sup>22,24</sup> In contrast, alkylidyne-imine chemistry is notably scarce and instead cycloadditions to the alkylidyne occur.<sup>28–31</sup> For example,<sup>29</sup> adding *N*-methyl-1-phenylmethanimine (PMI-Me) to cationic Mn complexes [Cp(CO)<sub>2</sub>Mn≡CR]<sup>+</sup> (R = Ph, Tol) produces the chelated alkylidene  $\eta^5$ -C<sub>5</sub>H<sub>4</sub>(CO)<sub>2</sub>Mn=C(R)N(CH<sub>3</sub>)C(H)Ph where the imine inserts into the Cp ligand. In contrast, combining the same PMI-Me with [Cp(CO)<sub>2</sub>Re≡CTol]<sup>+</sup> results in the [2+2] cycloaddition product (Scheme 1B). Activated alkynes also react with imines in metathesis-like reactions according to Scheme 1C.<sup>6,32–36</sup> However, missing from the catalogue is the metathesis between an

imine and an alkylidyne (Scheme 1D). In this study, we explore imine reactivity with strained and unstrained tungsten alkylidyne

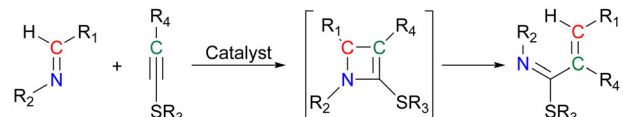
#### A. Alkylidene-Imine Metathesis



#### B. Alkylidyne-Imine Cycloaddition



#### C. Alkyne-Imine Metathesis



#### D. Alkylidyne-Imine Metathesis: This Work



**Scheme 1** (A) Alkylidene-imine metathesis with Nb, Ta, and Mo complexes. (B) Examples of alkylidyne-imine cycloaddition reactions. (C) Metathesis between activated alkynes and imines (D) Alkylidyne-imine metathesis (this work).

Department of Chemistry, Center for Catalysis, University of Florida, Gainesville, Florida, 32611, USA. E-mail: [veige@chem.ufl.edu](mailto:veige@chem.ufl.edu)

† Electronic supplementary information (ESI) available: NMR spectra, synthesis details. CCDC 2295329, 2295330, 2278025 and 2278026. For crystallographic data in CIF or other electronic format see DOI: <https://doi.org/10.1039/d3cc04583h>

complexes. The tungsten alkylidyne ( $^t\text{BuO})_3\text{W}\equiv\text{CC}(\text{CH}_3)_3$ <sup>37</sup> does not react with any imines examined even at elevated temperature. However, metathesis occurs between the trianionic pincer tungsten alkylidyne [ $^t\text{BuOCO}]W\text{CC}(\text{CH}_3)_3(\text{THF})_2$  (**1**)<sup>38</sup> and PMI-R imines.

Alkylidenes ring-open cyclic imines,<sup>22,27</sup> thus 3,4-dihydroisoquinoline (3,4-DHQ) was chosen to probe imine metathesis with alkylidenes. Treating complex **1** with one equiv. of 3,4-DHQ in benzene results in THF substitution and coordination of the imine to afford [ $^t\text{BuOCO}]W\equiv\text{CC}(\text{CH}_3)_3(3,4\text{-DHQ})$  (**2**) within 15 min. Maroon coloured crystals of **2** deposit at  $-30\text{ }^\circ\text{C}$  from a concentrated pentane or toluene solution within 2 d. Single crystal X-ray diffraction interrogation of the crystals provides the solid-state structure depicted in Fig. 1. The structure comprises the N-bound imine, the OCO pincer ligand and the intact alkylidyne. The complex is pseudo-*C*<sub>3</sub> symmetric with a plane of symmetry bisecting the complex through the W≡C alkylidyne and the imine ring. Presumably due to the strong

*trans* influence of the alkylidyne, the 3,4-DHQ coordinates in the *cis* position. Overall, the formally W(vi) ion adopts a distorted square pyramidal geometry with an Addison parameter<sup>39</sup> ( $\tau_5$ ) of 0.14. Complex **2** is thermally stable in solution at  $80\text{ }^\circ\text{C}$  for 2 d; metathesis does not occur.

The <sup>1</sup>H NMR spectrum of complex **2** is consistent with the solid-state *C*<sub>3</sub> structure. Two singlets for the pincer- $^t\text{Bu}$  and alkylidyne- $^t\text{Bu}$  protons appear at 1.57 and 0.70 ppm with relative integration of 2:1, respectively. The imine proton resonates as a singlet at 8.49 ppm. Diagnostic signals for the alkylidyne and *C*<sub>ipso</sub>-W carbons appear at 320.8 and 193.1 ppm, respectively. The imine carbon resonates at 171.8 ppm. Addition of less than one equiv. of 3,4-DHQ results in a portion of unreacted complex **1**. However, adding a slight excess of 3,4-DHQ results in an equilibrium mixture of **2**, free 3,4-DHQ, and a double substituted product where the alkylidyne inserts into the pincer backbone to give the tethered alkylidene complex [ $\text{O}_2\text{C}(^t\text{BuC}\equiv)]W(\eta^2\text{-3,4-DHQ})(3,4\text{-DHQ})$  (**3**) (Fig. 1).

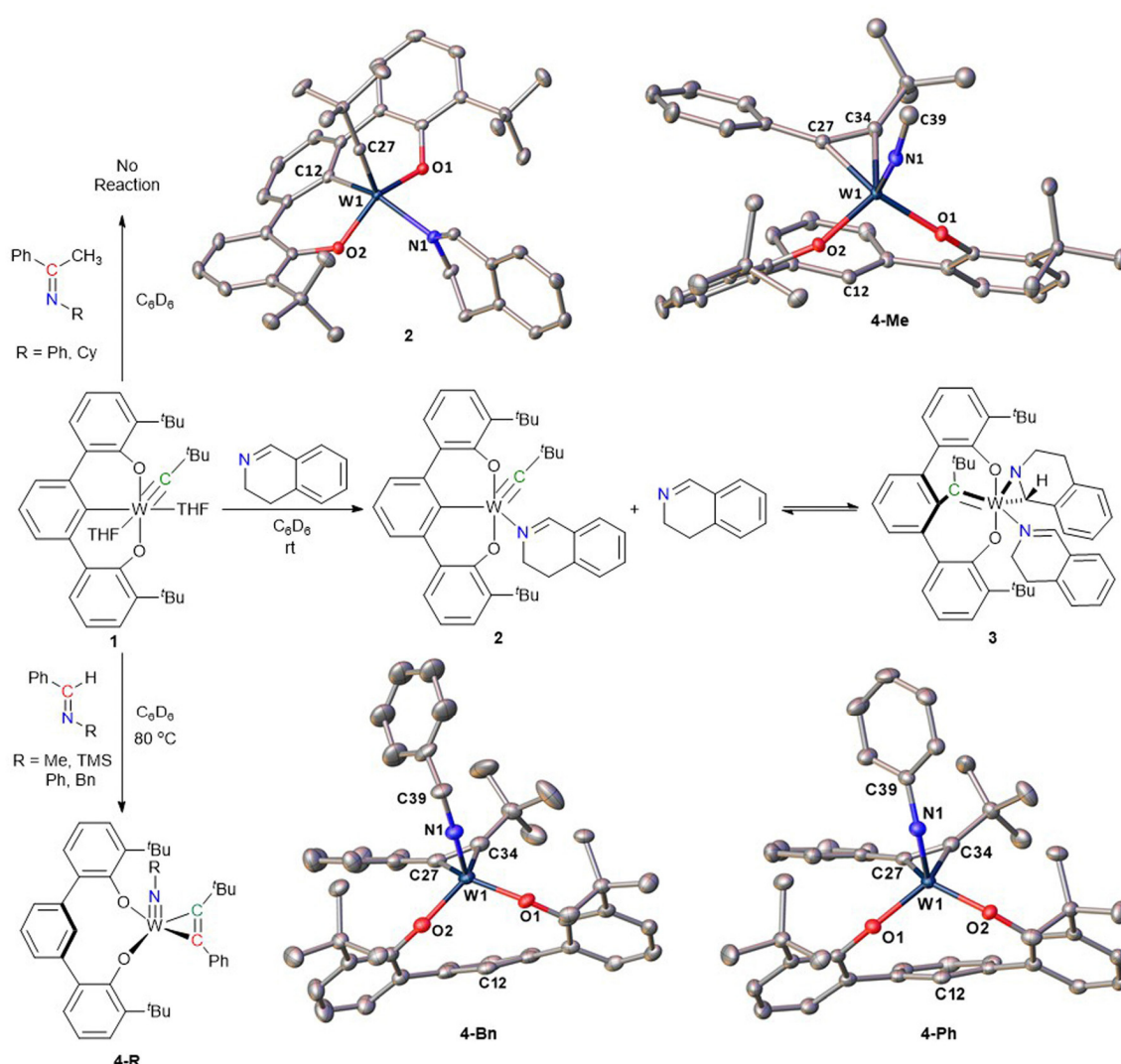


Fig. 1 Reactions between imines and complex **1** with solid state structures of **2** and **4-R**. Hydrogen atoms are omitted for clarity and thermal ellipsoid are presented at 50% probability.

Isolated solids of complex **2** show minor amounts of **3** are present by NMR spectroscopy. Adding 5 equiv. of 3,4-DHQ does not provide pure **3**. Instead, all three entities are identifiable *in situ* by NMR spectroscopy. The  $^1\text{H}$  NMR spectrum of the mixture reveals three singlets for the  $^t\text{Bu}$  groups of **3**, implying a  $C_1$  symmetric structure in solution. Aryl- $^t\text{Bu}$  protons reside at 1.50 and 1.04 ppm, and the alkylidene- $^t\text{Bu}$  protons resonate at 0.97 ppm with a 1:1:1 relative integration. The alkylidene and  $C_{ipso}$  carbon resonate at 256.3 and 118.1 ppm, respectively, drastically different from the monosubstituted complex **2** but consistent with known OCO supported tethered tungsten alkylidenes.<sup>40–44</sup> The  $^1\text{H}$ - $^1\text{H}$  and  $^1\text{H}$ - $^{13}\text{C}$  couplings in the homonuclear correlation spectroscopy (COSY), heteronuclear single quantum correlation (HSQC) and heteronuclear multiple bond correlation (HMBC) spectra identify the OCO ligand,  $^t\text{Bu}$ , DHQ and  $\eta^2$ -3,4-DHQ moieties (see ESI† for spectra). The nuclear Overhauser effects (nOes) between H29–31 of the  $\text{M}=\text{C}^t\text{Bu}$  group and H5, H14 and H24–26 on the OCO moiety provides evidence for a bond between C27 and C12 (Fig. 2). Providing evidence for an  $\eta^2$ -3,4-DHQ moiety, protons H29–31 display a strong nOe with H49 and H48 protons on the side of the DHQ facing the alkylidene, but only weak nOes to the opposite face. Another consequence of the  $\eta^2$ -3,4-DHQ is protons H29–31 do not exhibit an nOe with H41 since it points away. Also, the methine C41 exhibits an upfield signal at 44.7 ppm, consistent with being bound to W, whereas C32 resonates significantly downfield at 166.8 ppm. Indicating the DHQ coordinates in the assigned orientation in Fig. 2, only  $^t\text{Bu}$  protons H24–26 exhibit a nOe with the proximal H41. Interestingly, 3,4-DHQ binds in two different modes in the same complex. However, the binding modes themselves are not unusual and are previously reported in different complexes.<sup>40,41,43–45</sup> Reductive migratory insertion of the alkylidyne carbon into the W- $C_{ipso}$  bond is a common outcome when unsaturated substrates bind to complex **1**.<sup>40–44,46</sup> The insertion relaxes the constrained geometry enforced by the  $[\text{OCO}]^{3-}$  pincer ligand.

Though 3,4-DHQ only substitutes THF on complex **1**, PMI-R (*N*-methyl-1-phenylmethanimine, *N*-benzyl-1-phenylmethanimine, *N*-phenyl-1-phenylmethanimine, and *N*-trimethylsilyl-1-phenylmethanimine) execute metathesis.

Heating a dark red benzene solution of **1** with PMI-R imines at 80 °C for 2–4 d results in a colour change to transparent yellow signalling the formation of metathesis products  $[\text{BuO}-\text{C}(\text{H})\text{O}]W(\eta^2\text{-}^t\text{BuC}\equiv\text{CPh})\text{N}(\text{R})$  (**4-R**) in quantitative yield according

Table 1 Selected bond lengths (Å), bond angles (°), and geometric index for complexes **2**, **4-R**

	<b>2</b>	<b>4-Me</b>	<b>4-Ph</b>	<b>4-Bn</b>
W1-N1	2.210(16)	1.731(14)	1.757(19)	1.738(3)
W1-C27	1.763(17)	2.063(16)	2.034(2)	2.051(3)
W1-C34	—	2.047(17)	2.030(2)	2.044(3)
W1-C12	2.142(17)	—	—	—
C27-C34	—	1.325(2)	1.317(3)	1.322(5)
O1-W1-O2	144.38(5)	110.53(5)	109.51(6)	107.45(10)
C27-W1-C34	—	37.62(6)	37.84(9)	37.66(14)
W1-N1-C39	—	163.88(19)	148.98(17)	170.80(3)
$\tau_5$	0.14	0.01	0.02	0.02

to Fig. 1. Monitoring the reaction by NMR spectroscopy reveals complexes **4-R** begin to form within minutes but the distinct colour change only occurs as the reaction approaches completion. Complexes **4-Me** and **4-Bn** precipitate from concentrated pentane solution, and **4-Ph** and **4-TMS** precipitate from concentrated  $\text{Et}_2\text{O}$ : THF (9:1) solution as yellow crystals within 24 h at –30 °C. **4-R** are  $C_1$  symmetric in the solid state (Fig. 1). The structural parameters are similar for all the **4-R** complexes (Table 1). The formally W(vi) ion adopts a distorted square pyramidal geometry based on  $\tau_5$  values (Table 1).<sup>39</sup> The  $[\text{OCO}]^{3-}$  pincer is protonated to a dianionic  $[\text{OCO}]^{2-}$  ligand and resides in the basal plane. The metathesis product alkyne binds to the other two basal plane sites and the imido nitrogen occupies the axial position. Almost linear W1-N1-C39 bond angles and W1-N1 bond lengths (Table 1) agree with known tungsten imido complexes.<sup>43,47</sup> Consistent with a double bond and elongated to  $\approx 1.3$  Å, the C27-C34 bond lengths are consistent with published tungsten  $\eta^2$ -bound alkyne complexes.<sup>48–50</sup> NMR studies suggest that **4-R** retains  $C_1$  symmetry in solution as well, exhibiting three singlets attributable to the  $^t\text{Bu}$  protons in 1:1:1 relative integration ratio. The  $\eta^2$ -bound alkyne carbons appear upfield in the range 205 to 180 ppm as compared to alkylidene or alkylidyne carbons. A distinctive triplet signal appears  $\sim 8.00$  ppm for H12 in the  $^1\text{H}$  NMR spectrum.

The reaction between **1** and PMI-R imines is unprecedented. Reactions between alkylidenes and imines occur but none proceed through metathesis, instead cycloadditions occur.<sup>28–31</sup> The reaction between **1** and PMI-R imines is an alkylidene-imine metathesis reaction, as the exchange of fragments is evident within complexes **4-R**. The protonation of the pincer is critical to the reaction. Neither PMI-R imines nor 3,4-DHQ react with  $(^t\text{BuO})_3\text{W}\equiv\text{CC}(\text{CH}_3)_3$ , even upon heating. Exemplifying the need for protonation, *N*-cyclohexyl-1-phenylethan-1-imine and *N*-1-diphenylethan-1-imine, both lacking an acidic proton, do not react with complex **1** (Fig. 1).

In conclusion, two unusual reactivity outcomes occur upon treating complex **1** with imines. The constrained trianionic pincer ligand is critical to imparting the unusual reactivity. Using acyclic PMI-R imines, complex **1** executes a stoichiometric alkylidene-imine metathesis, clearly driven by protonation of the pincer backbone. Using cyclic 3,4-DHQ, complex **1** undergoes reductive migratory insertion into the pincer backbone to give tethered alkylidene **3**. Adding excess 3,4-DHQ to a solution of **1** induces reversible C–C bond cleavage between the tethered alkylidene **3** and alkylidyne **2**, but no metathesis occurs. An important conclusion from this work is that a masked active alkylidyne within complex **1** is

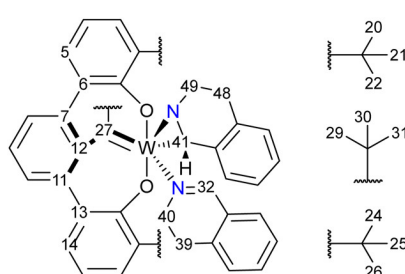


Fig. 2 Structure of complex **3** with relevant atom labels.

unleashed by protonating the backbone pincer. Studies elucidating the latency of the reactive alkylidyne in other metathesis reactions are ongoing.

This material is based upon work supported by the National Science Foundation CHE-2154377 (ASV), CHE-1828064 (KAA), CHE-0650456 (CENTC).

## Conflicts of interest

There are no conflicts to declare.

## References

- 1 M. E. Belowich and J. F. Stoddart, *Chem. Soc. Rev.*, 2012, **41**, 2003–2024.
- 2 R. Bloch, *Chem. Rev.*, 1998, **98**, 1407–1438.
- 3 C. D. Meyer, C. S. Joiner and J. F. Stoddart, *Chem. Soc. Rev.*, 2007, **36**, 1705–1723.
- 4 M. Ciaccia and S. Di Stefano, *Org. Biomol. Chem.*, 2015, **13**, 646–654.
- 5 G. K. Cantrell and T. Y. Meyer, *J. Am. Chem. Soc.*, 1998, **120**, 8035–8042.
- 6 R. T. Ruck, R. L. Zuckerman, S. W. Krska and R. G. Bergman, *Angew. Chem., Int. Ed.*, 2004, **43**, 5372–5374.
- 7 H. Vardhan, A. Mehta, I. Nath and F. Verpoort, *RSC Adv.*, 2015, **5**, 67011–67030.
- 8 A. Liguori and M. Hakkarainen, *Macromol. Rapid Commun.*, 2022, **43**, 2100816.
- 9 J. Ahner, M. Micheel, R. Geitner, M. Schmitt, J. Popp, B. Dietzek and M. D. Hager, *Macromolecules*, 2017, **50**, 3789–3795.
- 10 Y. Lun, Y. Zang, T. Aoki, M. Teraguchi and T. Kaneko, *Chem. Lett.*, 2017, **46**, 401–404.
- 11 J. M. McInnes, A. J. Blake and P. Mountford, *J. Chem. Soc., Dalton Trans.*, 1998, 3623–3628.
- 12 K. E. Meyer, P. J. Walsh and R. G. Bergman, *J. Am. Chem. Soc.*, 1994, **116**, 2669–2670.
- 13 G. K. Cantrell and T. Y. Meyer, *Organometallics*, 1997, **16**, 5381–5383.
- 14 J. M. McInnes and P. Mountford, *Chem. Commun.*, 1998, 1669–1670.
- 15 J. W. Bruno and X. J. Li, *Organometallics*, 2000, **19**, 4672–4674.
- 16 M. A. Aljuhani, S. Barman, E. Abou-Hamad, A. Gurinov, S. Ould-Chikh, E. Guan, A. Jedidi, L. Cavallo, B. C. Gates, J. D. A. Pelletier and J. M. Basset, *ACS Catal.*, 2018, **8**, 9440–9446.
- 17 M. A. Aljuhani, J. D. A. Pelletier and J. M. Basset, *J. Visualized Exp.*, 2019, **2019**, 1–11.
- 18 M. Bühl, *Chem. – Eur. J.*, 1999, **5**, 3514–3522.
- 19 J.-L. Hérisson and Y. Chauvin, *Makromol. Chem.*, 1970, **141**, 161–176.
- 20 M. Bühl, *J. Mol. Model.*, 2000, **6**, 112–118.
- 21 M. C. Burland, T. Y. Meyer and M. H. Baik, *J. Org. Chem.*, 2004, **69**, 6173–6184.
- 22 G. K. Cantrell, S. J. Geib and T. Y. Meyer, *Organometallics*, 2000, **19**, 3562–3568.
- 23 S. M. Rocklage and R. R. Schrock, *J. Am. Chem. Soc.*, 1980, **102**, 7808–7809.
- 24 S. M. Rocklage and R. R. Schrock, *J. Am. Chem. Soc.*, 1982, **104**, 3077–3081.
- 25 C. K. Murray, B. P. Warner, V. Dragisich, W. D. Wulff and R. D. Rogers, *Organometallics*, 1990, **9**, 3142–3151.
- 26 H. Fischer, A. Schlageten, W. Bidell and A. Früh, *Organometallics*, 1991, **10**, 389–391.
- 27 G. K. Cantrell, S. J. Geib and T. Y. Meyer, *Organometallics*, 1999, **18**, 4250–4252.
- 28 M. R. Terry, L. A. Mercando, C. Kelley, G. L. Geoffroy, P. Nombel, N. Lugar, R. Mathieu, R. L. Ostrander, B. E. Owens-Waltermire and A. L. Rheingold, *Organometallics*, 1994, **13**, 843–865.
- 29 B. M. Handwerker, K. E. Garrett, K. L. Nagle, G. L. Geoffrey and A. L. Rheingold, *Organometallics*, 1990, **9**, 1562–1575.
- 30 B. M. Handwerker, K. E. Garrett, G. L. Geoffrey and A. L. Rheingold, *J. Am. Chem. Soc.*, 1989, **111**, 369–371.
- 31 Y. Tang, J. Sun and J. Chen, *Organometallics*, 1999, **18**, 2459–2465.
- 32 H. Ishitani, S. Nagayama and S. Kobayashi, *J. Org. Chem.*, 1996, **61**, 1902–1903.
- 33 Y. Ma and C. Qian, *Tetrahedron Lett.*, 2000, **41**, 945–947.
- 34 M. Shindo, S. Oya, R. Murakami, Y. Sato and K. Shishido, *Tetrahedron Lett.*, 2000, **41**, 5947–5950.
- 35 H. Aneetha, F. Basuli, J. Bollinger, J. C. Huffman and D. J. Mindiola, *Organometallics*, 2006, **25**, 2402–2404.
- 36 A. Saito, J. Kasai, T. Konishi and Y. Hanzawa, *J. Org. Chem.*, 2010, **75**, 6980–6982.
- 37 M. L. Listemann and R. R. Schrock, *Organometallics*, 1985, **4**, 74–83.
- 38 S. Sarkar, K. P. McGowan, S. Kuppuswamy, I. Ghiviriga, K. A. Abboud and A. S. Veige, *J. Am. Chem. Soc.*, 2012, **134**, 4509–4512.
- 39 A. W. Addison, T. N. Rao, J. Reedijk, J. Van Rijn and G. C. Verschoor, *J. Chem. Soc., Dalton Trans.*, 1984, **0**, 1349–1356.
- 40 K. P. McGowan, M. E. O'reilly, I. Ghiviriga, K. A. Abboud and A. S. Veige, *Chem. Sci.*, 2013, **4**, 1145–1155.
- 41 C. D. Roland, H. Li, K. A. Abboud, K. B. Wagener and A. S. Veige, *Nat. Chem.*, 2016, **8**, 791–796.
- 42 S. A. Gonsales, T. Kubo, M. K. Flint, K. A. Abboud, B. S. Sumerlin and A. S. Veige, *J. Am. Chem. Soc.*, 2016, **138**, 4996–4999.
- 43 V. Jakhar, D. Pal, I. Ghiviriga, K. A. Abboud, D. W. Lester, B. S. Sumerlin and A. S. Veige, *J. Am. Chem. Soc.*, 2021, **143**, 1235–1246.
- 44 S. S. Nadif, T. Kubo, S. A. Gonsales, S. VenkatRamani, I. Ghiviriga, B. S. Sumerlin and A. S. Veige, *J. Am. Chem. Soc.*, 2016, **138**, 6408–6411.
- 45 V. K. Jakhar, A. M. Esper, I. Ghiviriga, K. A. Abboud, C. Ehm and A. S. Veige, *Angew. Chem., Int. Ed.*, 2022, **61**, e202203073.
- 46 V. K. Jakhar, A. M. Esper, I. Ghiviriga, K. A. Abboud, C. Ehm and A. S. Veige, *Angew. Chem.*, 2022, **134**, 2–9.
- 47 C. R. Clough, J. B. Greco, J. S. Figueroa, P. L. Diaconescu, W. M. Davis and C. C. Cummins, *J. Am. Chem. Soc.*, 2004, **126**, 7742–7743.
- 48 S. M. Holmes, D. F. Schafer, P. T. Wolczanski and E. B. Lobkovsky, *J. Am. Chem. Soc.*, 2001, **123**, 10571–10583.
- 49 R. J. Beattie, P. S. White and J. L. Templeton, *Organometallics*, 2016, **35**, 32–38.
- 50 T. W. Hayton, J. M. Boncella, B. L. Scott, K. A. Abboud and R. C. Mills, *Inorg. Chem.*, 2005, **44**, 9506–9517.